EPD Congress 2015
Edited by: James Yurko, Antoine Allanore, Laura Bartlett, Jonghyun Lee, Lifeng Zhang, Gabriella Tranell, Yulia Meteleva-Fischer, Shadia Ikhmayies, Arief Suriadi Budiman, Prabhat Tripathy, and Guy Fredrickson
TMS (The Minerals, Metals & Materials Society), 2015

SYNTHESIS OF HIGH PERFORMANCE $LiMn_{0.8}Fe_{0.2}PO_4$/C CATHODE MATERIAL FOR LITHIUM ION BATTERIES: EFFECT OF CALCINATION TEMPERATURE

Enrui Dai [1,2], Weibing Chen [1,2], Haisheng Fang [1,2,*], Hui Wang [3], Bin Yang [1,2,*], Wenhui Ma [1,2]

[1]State Key Laboratory of Complex Nonferrous Metal Resources Clean Utilization, Kunming University of Science and Technology, Kunming 650093, China
[2]Key Laboratory of Nonferrous Metals Vacuum Metallurgy of Yunnan Province, Kunming University of Science and Technology, Kunming 650093, China
[3]Technical Institute of Physics and Chemistry, Chinese Academy of Sciences, Beijing 100190, China

Keywords: Lithium ion batteries; Cathode material; Lithium manganese phosphate

Abstract

$LiMn_{0.8}Fe_{0.2}PO_4$/C composite was prepared by an improved solid-state method and the effect of calcination temperature on properties of the obtained materials was investigated. The results showed that increasing calcination temperature from 600 to 700 ^oC improved the performance of the $LiMn_{0.8}Fe_{0.2}PO_4$/C due to enhanced crystallinity and increased conductivity, but further increase in calcination temperature to 800 ^oC led to degraded performance due to particle growth and decrease in porosity. Therefore, the $LiMn_{0.8}Fe_{0.2}PO_4$/C composite prepared at 700 ^oC exhibited the best electrochemical performance, and could deliver a high capacity of 152 mAh g^{-1} at 0.1 C, 147 mAh g^{-1} at 1 C and 114 mAh g^{-1} at 10 C. In addition, the performance of the $LiMn_{0.8}Fe_{0.2}PO_4$/C and $LiMn_{0.8}Fe_{0.19}Mg_{0.01}PO_4$/C was compared when they were obtained at the optimum calcination temperature.

Introduction

As a cathode material for lithium ion batteries, olivine structured $LiMnPO_4$ has received increasing attention because of its good cyclic performance, excellent chemical and thermal stabilities, low toxicity and low cost. It offers a redox potential of 4.1 V vs. Li^+/Li, which means a higher energy density as compared to that of $LiFePO_4$ (3.4 V vs. Li^+/Li) [1]. However, previous studies showed that the kinetic behavior of $LiMnPO_4$ is too poor to show any reversible capacity [2]. Several approaches have been adopted to improve the performance of $LiMnPO_4$: preparing smaller particles [3-9], carbon coating [10-12] and cation substitution [13-16]. However, no matter whichever approach is used, the improvement of the performance is critically dependent on synthesis method. Recently, we have developed an improved solid-state method to synthesize both pure $LiMnPO_4$/C and substituted $LiMnPO_4$/C where Mn was substituted by Zn, Mg and Mg+Fe. The resultant materials showed good electrochemical performance. In the year of 2010 we reported that the Fe&Mg co-substituted $LiMnPO_4$/C showed better electrochemical performance than the Fe substituted $LiMnPO_4$/C when they were prepared by the same method at the same calcination temperature (800 ^oC) [17], but more recently we found out that the optimum calcination temperature may be different for substituted $LiMnPO_4$ even if they were prepared by the same method. For example, the Zn or Mg substituted $LiMnPO_4$/C showed the best

* Corresponding author. Tel. / fax: +86 871 65107208.
E-mail address: hsfang1981@hotmail.com (H.S. Fang), kgyb2005@126.com (B. Yang).

performance at 700 ^{o}C [18], while the Fe&Mg co-substituted $LiMnPO_4$/C had the optimum performance at 800 ^{o}C [19]. Now the question arises as to whether there is a difference in the optimum calcination temperature between Fe and Fe-Mg substituted $LiMnPO_4$/C and if so does the latter show better performance over the former when both are synthesized at the same (optimum) calcination temperature? If this is the case, then the question is whether the performance of the Fe&Mg co-substituted $LiMnPO_4$/C is still better than that of the Fe substituted $LiMnPO_4$/C when they are obtained at the optimal calcination temperature. The paper describes a new solid state synthesis process for $LiMn_{0.8}Fe_{0.2}PO_4$/C and how the calcination temperature helped improve its performance characteristics. Moreover, the performance of the $LiMn_{0.8}Fe_{0.2}PO_4$/C and $LiMn_{0.8}Fe_{0.19}Mg_{0.01}PO_4$/C is compared when they are obtained at the optimal calcination temperature. The objective of this investigation was two-fold: to verify if the (i) new preparative approach can yield high performance $LiMn_{0.8}Fe_{0.2}PO_4$/C and (ii) Fe&Mg co-substitution is better than just the Fe substitution!

Experimental

High purity LiH_2PO_4, $MnC_4H_6O_4{\cdot}4H_2O$, $H_2C_2O_4{\cdot}2H_2O$ and $FeC_2O_4{\cdot}2H_2O$ in the mole ratio of 1:0.8:0.8:0.2 were mixed and homogenized with ~7 wt.% sucrose in a ball miller for 6 h. During ball-milling process, the oxalic acid induced a room temperature solid-state reaction with $MnC_4H_6O_4{\cdot}4H_2O$ to form nanosize $MnC_2O_4{\cdot}2H_2O$. The milled mixture was dried and then heated (heating rate: 2 ^{o}C min^{-1}) to 600-800 ^{o}C for 10 h under Ar atmosphere.
Powder XRD (D/MaX-3, Rigaku) technique was used to identify the product phases. Lattice parameters of different phases were determined by the refinement of the XRD patterns using silicon (99.9% pure) as the internal standard. Powder morphology and particle size distribution were measured by SEM (XL30, Phillips) and TEM (Tecnai G2 F20, FEI) respectively. The total carbon content was determined by a carbon analyzer (VarioEL III elementar). The surface area and pore size distribution were estimated by a surface adsorption analyzer (NOVA2200e, Quantachrome instrument) using nitrogen as the carrier gas. The electronic conductivity was determined by a four-point resistivity measurement probe (RTS-8, Four Probes Tech.). The samples for the conductivity measurement were prepared in the form of discs by manually pressing the powder under an applied load of 20MPa. Electrochemical measurements were carried out with CR2025 coin cells and lithium metal as the anode. The cathode was prepared in the form of a slurry by mixing the synthesized powder, super P (that is conductive carbon black), and polyvinylidene fluoride (PVDF) (in the ratio 8:1:1) in N-methyl pyrrolidinone (NMP). The slurry was coated with an aluminum foil using a doctor blade coater. The diameter and active mass of the cathode were 1.3 cm and ~2.3mg respectively. 1M $LiPF_6$ in EC/DMC (1:1 ratio) was used as the electrolyte. The electrochemical cell was assembled in an argon-atmosphere glove box and the measurements were carried out under both constant current as well as voltage modes during charging and constant current mode during discharging, using a battery test system (Land CT2001A) at 30 ^{o}C.

Results and discussion

Fig. 1 shows the XRD pattern of the synthesized $LiMn_{0.8}Fe_{0.2}PO_4$/C at different temperatures. All samples were observed to have similar patterns that can be indexed into an orthorhombic structure with a space group of *Pmnb*. The diffraction peaks become more intense with increasing temperature, indicating enhanced crystallinity of the samples at higher temperatures. The refinement of XRD patterns revealed that the lattice parameters of these samples varied negligibly with the temperature, and all were around a = 6.0822 Å, b = 10.4253 Å and c =

4.7318 Å. Besides, the absence of carbon peak in the XRD patterns indicated the formation of amorphous residual carbon by way of pyrolysis of sucrose. Relatively higher temperatures led to an apparent decrease in the carbon content in the composite. However, electronic conductivity increased with an increase in the temperature, which can be attributed to the enhanced electronic conductivity of the residual carbon since raising pyrolysis temperature above 700 ^{o}C can dramatically increase the electronic conductivity of the carbon film [20]. These observations suggest that the quality of carbon is more important than its quantity. The carbon content and electronic conductivity of the $LiMn_{0.8}Fe_{0.2}PO_4$/C prepared at different temperatures are listed in Table 1.

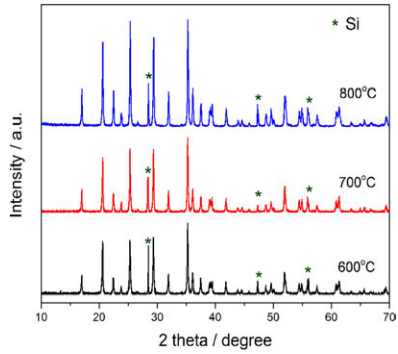

Figure 1. XRD patterns of $LiMn_{0.8}Fe_{0.2}PO_4$/C synthesized at different temperatures. The asterisk (*) denotes the internal silicon standard.

Table 1. Carbon content and electronic conductivity of $LiMn_{0.8}Fe_{0.2}PO_4$/C synthesized at different calcination temperatures.

Calcination temperature (^{o}C)	Carbon content (wt.%)	Electronic conductivity (S cm^{-1})
600	9.05	1.3×10^{-4}
700	7.32	1.1×10^{-2}
800	6.64	2.5×10^{-2}

Fig. 2 presents the SEM images of $LiMn_{0.8}Fe_{0.2}PO_4$/C synthesized at different temperatures. All samples showed a similar morphology with primary particles being agglomerated together. Increased (from 600-700 ^{o}C) did not cause obvious coarsening of primary particles, but temperatures > 800 ^{o}C led to an apparent increase in the primary particles size. The TEM images (Fig. 3) of $LiMn_{0.8}Fe_{0.2}PO_4$/C samples showed a porous structure of aggregate particles which have also been observed by others for $LiMnPO_4$ composites, prepared by the same route [21-22]. Formation of such a porous structure has demonstrated to be crucial for the electrochemical performance [21]. Moreover, the coarsening of primary particles was observed for the samples prepared at 800 ^{o}C, which is similar to the SEM observation.

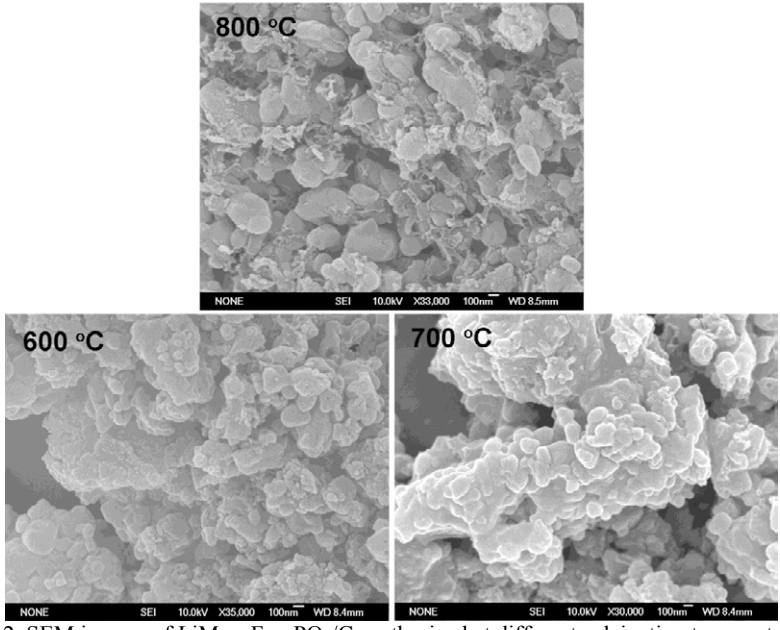

Figure 2. SEM images of $LiMn_{0.8}Fe_{0.2}PO_4/C$ synthesized at different calcination temperatures.

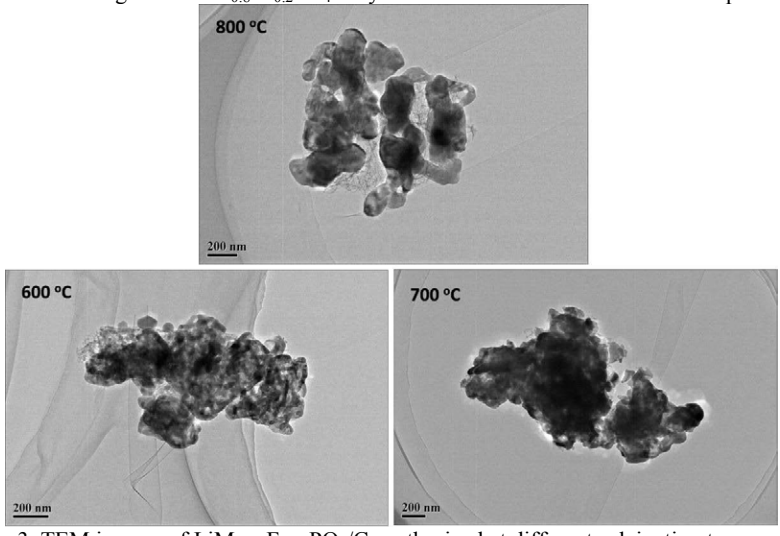

Figure 3. TEM images of $LiMn_{0.8}Fe_{0.2}PO_4/C$ synthesized at different calcination temperatures.

Fig. 4 represents N_2 adsorption and desorption isotherms of $LiMn_{0.8}Fe_{0.2}PO_4/C$ synthesized at different temperatures. All isotherms are of type IV with type H3 hysteresis loops at the higher P/P_o ratio [23], indicating the existence of non-uniform and slit-shaped mesopores. The surface area of the samples, synthesized at 600, 700 and 800 ^oC were estimated to be 51.5, 45.1 and 25.8

$m^2\ g^{-1}$, respectively. The dramatic decrease of the surface area of the sample prepared at 800 °C meant a rapid growth of primary particles. Interestingly, our previous study showed that there was no evidence of the growth of the particles for Fe&Mg co-substituted $LiMnPO_4$/C prepared by the same method in the temperature range 600-800 °C [24]. Considering the particle-size dependent performance of $LiMnPO_4$ based material, such a difference may result in a different optimal calcination temperature between the Fe substituted $LiMnPO_4$/C and the Fe&Mg co-substituted $LiMnPO_4$/C. Besides the particle size change, the N_2 adsorption measurement also revealed a variation in the porosity of the three samples. Based on the Barrett – Joyner – Halenda (BJH) method, the derived surface area of the samples synthesized at 600, 700 and 800 °C was determined to be 52.8, 45 and 35.1 $m^2\ g^{-1}$, respectively. The measurement of the BJH surface area was determined based on the capillary condensation in pores and thus this result indicated that the porosity of samples decreased with the increase in calcination temperature. Indeed, the pore volume of the samples synthesized at 600, 700 and 800 °C decreased to 0.185, 0.160 to 0.133 $m^3\ g^{-1}$, respectively. These results are consistent with the SEM and TEM observations. Our previous work has proved that the presence of sufficient porosity is essential to achieve high performance of $LiMnPO_4$ based material [21].

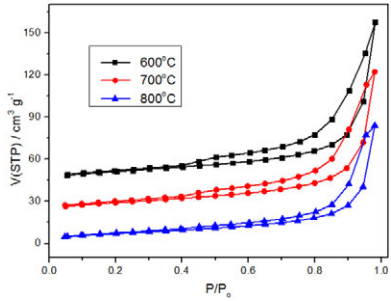

Figure 4. N_2 adsorption and desorption isotherms of $LiMn_{0.8}Fe_{0.2}PO_4$/C synthesized at different calcination temperatures.

Fig. 5a shows the typical charging and discharging curves obtained for $LiMn_{0.8}Fe_{0.2}PO_4$/C synthesized at different calcination temperatures. Cells were charged at 0.2 C (equal to 30 mA g^{-1}) to 4.5 V, held at 4.5 V until the current decreased to 0.02 C, and then discharged at 0.2 C to 2.5 V. As can be seen in Fig. 5a, the charging-discharging plateaus around 4.1 V are related to the Mn^{3+}/Mn^{2+} redox couple, and the plateaus around 3.4 V are related to the Fe^{3+}/Fe^{2+} redox couple. Although all samples exhibited similar charging/discharging profiles, it is clear that the $LiMn_{0.8}Fe_{0.2}PO_4$/C synthesized at 700 °C showed a much higher reversible capacity as compared to other two samples. The specific discharge capacities at 0.2 C were 139 mAh g^{-1}, 150 mAh g^{-1} and 128 mAh g^{-1} for the $LiMn_{0.8}Fe_{0.2}PO_4$/C synthesized at 600, 700 and 800 °C, respectively. Moreover, all samples exhibited good cycling performance as shown in Fig.5b, and only tiny capacity loss was observed after 50 cycles, especially for the $LiMn_{0.8}Fe_{0.2}PO_4$/C prepared at 700 °C.

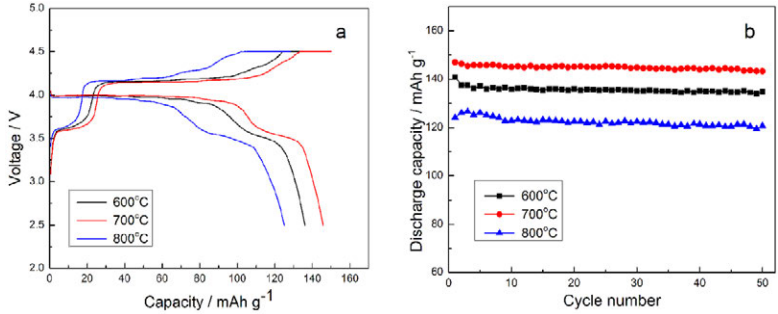

Figure 5. (a) Charging/discharging curves of $LiMn_{0.8}Fe_{0.2}PO_4/C$ synthesized at different calcination temperatures cycled at 0.2 C (equal to 30 mA g^{-1}). (b) Cycling performance of $LiMn_{0.8}Fe_{0.2}PO_4/C$ synthesized at different calcination temperatures cycled at 0.2 C. Cells were charged at 0.2 C to 4.5 V, held at 4.5 V until the current decreased to 0.02 C, and then discharged at 0.2 C to 2.5 V.

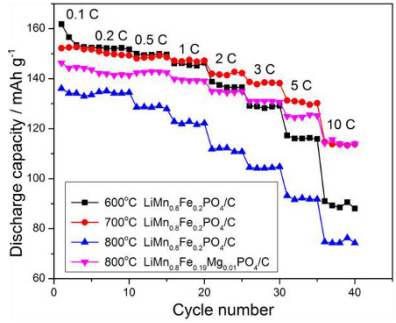

Figure 6. Rate performance of $LiMn_{0.8}Fe_{0.2}PO_4/C$ synthesized at different calcination temperatures and $LiMn_{0.8}Fe_{0.19}Mg_{0.01}PO_4/C$ synthesized at 800 °C. Cells were charged at 0.1 C to 4.5 V, held at 4.5V until the current decreased to 0.01 C, and then discharged at various rates to 2.0 V.

Fig. 6 depicts the rate performance of $LiMn_{0.8}Fe_{0.2}PO_4/C$ synthesized at different calcination temperatures. Cells were charged at 0.1 C to 4.5 V, held at 4.5 V until the current decreased to 0.01 C, and then discharged at various rates to 2 V. It is evident that the $LiMn_{0.8}Fe_{0.2}PO_4/C$ synthesized at 700 °C showed the best rate capability. The reversible capacity could reach 152 mAh g^{-1} at 0.1 C, 147 mAh g^{-1} at 1 C, 142 mAh g^{-1} at 2 C, 138 mAh g^{-1} at 3 C, 131 mAh g^{-1} at 5 C and 114 mAh g^{-1} at 10 C. There have been many reports on the synthesis of $LiMn_{0.8}Fe_{0.2}PO_4/C$. For example, Martha et al. communicated that carbon-coated $LiMn_{0.8}Fe_{0.2}PO_4$ nanoparticles synthesized by a solid-state reaction could deliver a reversible capacity of 165 mAh g^{-1} at 1/20 C and 100 mAh g^{-1} at 10 C [24]. Huang et al. reported a carbon coated mesoporous $LiMn_{0.8}Fe_{0.2}PO_4$ solid solution which could discharge a capacity of 140 mAh g^{-1} at 1/20 C and 80 mAh g^{-1} at 2 C [25]. Du et al. reported that a reversible capacity of 151.1 mAh g^{-1} at 0.1 C, 98.4 mAh g^{-1} at 5 C and 82 mAh g^{-1} at 10 C could be achieved for $LiMn_{0.8}Fe_{0.2}PO_4/C$ prepared by a co-precipitation method [26]. Evidently, the $LiMn_{0.8}Fe_{0.2}PO_4/C$ prepared at 700 °C by us exhibited better performance than all the values reported in literatures thus far.

Thus all the above experimental studies indicated that the better performance characteristics of $LiMn_{0.8}Fe_{0.2}PO_4$/C could be achieved with increasing calcination temperature from 600 to 700 ^oC because of the enhanced crystallinity and increased conductivity at 700 ^oC. The degradation in the performance of the sample, prepared at 800 ^oC, could be correlated to the coarsening of the particle resulting in a decrease in the porosity. Studies also revealed that the particle size distribution and higher conductivity (because of amorphous carbon coating) are two important parameters responsible for the improvement in performance. Besides, careful experimentation revealed that while the optimum temperatures for (i) $LiMn_{0.8}Fe_{0.2}PO_4$/C, and (ii) Zn/Mg substituted $LiMnPO_4$/C) to be 700 ^oC, the value for Fe&Mg co-substitution was determined to be 800 ^oC [19]. It was also observed that the Fe&Mg co-substitution ($LiMn_{0.8}Fe_{0.19}Mg_{0.01}PO_4$/C with ~7 wt.% C) showed somewhat lower capacity than the compound without Mg ($LiMn_{0.8}Fe_{0.2}PO_4$/C) when the rate was $\leq$ 5 C but almost has the same capacity at 10 C. This suggests that the Fe&Mg co-substitution can demonstrate superior performance characteristics, over just Fe substitution, at higher rates.

Scale up studies may be performed to establish the superiority of the co-substitution (Fe with Mg) with a view to designing the $LiMnPO_4$ based cathode materials for high power lithium ion batteries.

Conclusions

$LiMn_{0.8}Fe_{0.2}PO_4$/C composite was prepared by a solid-state method at different calcination temperatures. The lattice parameters of $LiMn_{0.8}Fe_{0.2}PO_4$ changed slightly with calcination temperature, but the conductivity, particle size and porosity of the $LiMn_{0.8}Fe_{0.2}PO_4$/C were strongly dependent on the calcination temperature. The $LiMn_{0.8}Fe_{0.2}PO_4$/C obtained at 700 ^oC had the best electrochemical performance with a discharge capacity of 152 mAh g^{-1} at 0.1 C and 114 mAh g^{-1} at 10 C. However, the $LiMn_{0.8}Fe_{0.2}PO_4$/C still showed a relatively faster capacity fade at high rates as compared to the $LiMn_{0.8}Fe_{0.19}Mg_{0.01}PO_4$/C.

Acknowledgements

This work was supported by the National Natural Science Foundation of China (No. 51304098), the Specialized Research Fund for the Doctoral Program of Higher Education (No. 20125314120004) and the Program for Innovative Research Team in University of Ministry of Education of China (No. IRT1250).

References

[1] A.K. Padhi, K.S. Nanjundaswamy, et al., "Phospho-olivines as Positive Electrode Materials for Rechargeable lithium batteries," *J. Electrochem. Soc.* 144 (1997), 1188-1194.

[2] M. Yonemura, A. Yamada, et al., "Comparative Kinetic Study of Olivine Li_xMPO_4 (M = Fe, Mn)," *J. Electrochem. Soc.* 151 (2004), A1352-A1356.

[3] Z. Bakenov, I. Taniguchi, "Electrochemical performance of nanocomposite $LiMnPO_4$/C cathode materials for lithium batteries," *Electrochem. Commun.* 12 (2010), 75-78.

[4] J. Xiao, W. Xu, et al., "Synthesis and Characterization of Lithium Manganese Phosphate by a Precipitation Method," *J. Electrochem. Soc.* 157 (2010), A142-A147.

[5] D. Wang, H. Buqa, et al., "High-performance, nano-structured $LiMnPO_4$ synthesized via a polyol method," *J. Power Sources* 189 (2009), 624-628.

[6] D. Choi, D. Wang, et al., "$LiMnPO_4$ nanoplate grown via solid-state reaction in molten hydrocarbon for Li-ion battery cathode," *Nano Lett.* 10 (2010), 2799-2805.

[7] H. Ji, G. Yang, et al., "General synthesis and morphology control of $LiMnPO_4$ nanocrystals via microwave-hydrothermal route," *Electrochim. Acta* 56 (2011), 3093-3100.
[8] K.T. Lee, J. Cho, "Roles of nanosize in lithium reactive nanomaterials for lithium ion batteries," *Nano Today* 6 (2011), 28-41.
[9] Y. Dong, L. Wang, et al., "Two-phase interface in $LiMnPO_4$ nanoplates," *J. Power Sources* 215 (2012), 116-121.
[10] C. Delacourt, P. Poizot, et al., "One-Step Low-Temperature Route for the Preparation of Electrochemically Active $LiMnPO_4$ Powders," *Chem. Mater.* 16 (2004), 93-99.
[11] S.M. Oh, S.W. Oh, et al., "High-Performance Carbon-$LiMnPO_4$ Nanocomposite Cathode for Lithium Batteries," *Adv. Funct. Mater.* 20 (2010), 3260-3265.
[12] Z. Bakenov, I. Taniguchi, "Physical and electrochemical properties of $LiMnPO_4$/C composite cathode prepared with different conductive carbons," *J. Power Sources* 195 (2010), 7445-7451.
[13] T. Shiratsuchi, S. Okada, et al., "Cathodic performance of $LiMn_{1-x}M_xPO_4$ (M = Ti, Mg and Zr) annealed in an inert atmosphere," *Electrochim. Acta* 54 (2009), 3145-3151.
[14] J.W. Lee, M.S. Park, et al., "Electrochemical lithiation and delithiation of $LiMnPO_4$: Effect of cation substitution," *Electrochim. Acta* 55 (2010), 4162-4169.
[15] J. Kim, D.H. Seo, et al., "Mn based olivine electrode material with high power and energy," *Chem. Commun.* 46 (2010), 1305-1307.
[16] G. Yang, H. Ni, et al., "The doping effect on the crystal structure and electrochemical properties of $LiMn_xM_{1-x}PO_4$ (M = Mg, V, Fe, Co, Gd)," *J. Power Sources* 196 (2011), 4747-4755.
[17] C.L. Hu, H.H. Yi, et al., "Improving the electrochemical activity of $LiMnPO_4$ via Mn-site co-substitution with Fe and Mg," *Electrochem. Commun.* 12 (2010), 1784-1787.
[18] H.S. Fang, H.H. Yi, et al., Unpublished Results.
[19] H.H. Yi, C.L. Hu, et al., "Optimized electrochemical performance of $LiMn_{0.9}Fe_{0.1-x}Mg_xPO_4$/C for lithium ion batteries," *Electrochim. Acta* 56 (2011), 4052-4057.
[20] R. Kostecki, B. Schnyder, et al., "Surface studies of carbon films from pyrolyzed photoresist," *Thin Solid Films* 396 (2001), 36-43.
[21] H.S. Fang, Y.J. Hu, et al., "The essential role of aggregate porosity in improving the performance of $LiMnPO_4$/C," *Electrochim. Acta* 106 (2013), 215-218.
[22] S. Liu, H.S. Fang, et al., "Effect of carbon content on properties of $LiMn_{0.8}Fe_{0.19}Mg_{0.01}PO_4$/C composite cathode for lithium ion batteries," *Electrochim. Acta* 116 (2014), 97-102.
[23] K.S.W. Sing, D.H. Everett, et al., "Reporting physisorption data for gas/solid systems with special reference to the determination of surface area and porosity," *Pure Appl. Chem.* 57 (1985), 603-619.
[24] S.K. Martha, J. Grinblat, et al., "$LiMn_{0.8}Fe_{0.2}PO_4$: an advanced cathode material for rechargeable lithium batteries," *Angew. Chem. Int. Ed.* 48 (2009), 8559-8563.
[25] B. Zhang, X.J. Wang, et al., "Enhanced Electrochemical Performances of Carbon Coated Mesoporous $LiFe_{0.2}Mn_{0.8}PO_4$," *J. Electrochem. Soc.* 157 (2010), A285- A288.
[26] K. Du, L.H. Zhang, et al., "Synthesis of $LiMn_{0.8}Fe_{0.2}PO_4$/C by co-precipitation method and its electrochemical performances as a cathode material for lithium-ion batteries," *Mater. Chem. Phys.* 136 (2012), 925-929.
[27] J. Wolfenstine, U. Lee, et al., "Electrical conductivity and rate-capability of $Li_4Ti_5O_{12}$ as a function of heat-treatment atmosphere," *J. Power Sources* 154 (2006), 287-289.